LH$_2$ Target Density in Hall A Experiment E01-020

P.E. Ulmer

Department of Physics
Old Dominion University
Norfolk, VA 23529
E-mail: pulmer@odu.edu

Experiment E01-020 [1] consisted of a measurement of the ^{2}H$(e, e'p)$n cross section over a broad kinematical phase space using the Hall A [2] high resolution spectrometer pair. In order to calibrate our kinematics and check our cross section normalization, we measured elastic scattering in ^{1}H$(e, e'p)$ using a 15 cm liquid hydrogen target with the "cigar-tube" cell. The normalization check involves knowledge of the liquid hydrogen density seen by the beam. In this paper, I show the results of a study of target density performed at fixed beam energy and with the high resolution spectrometers at fixed kinematics for varying beam current. For this study a "nominal" 2 mm × 2 mm square beam raster was used with the target fan frequency set to 60 Hz. For beam currents above 40 μA the density falls off linearly with beam current and also with position along the beam. No significant reduction was found near the entrance of the target cell even for the highest beam current employed, 111 μA. Below 40 μA, no significant density reduction was found.

1 Introduction

Hall A Experiment E01-020 ($(e, e'p)$ *Studies of the Deuteron at High Q^2*) [1] employed the 15 cm cigar-tube target cells. One cell was filled with liquid deuterium for the production data, while another was filled with liquid hydrogen, for kinematics and normalization checks. In order to check the hydrogen normalization we studied the dependence of the liquid hydrogen (LH$_2$) density on beam current for fixed kinematics. During this study the beam was rastered over a nominally 2 mm × 2 mm spot, the same raster size used for the production data on deuterium. See the next section for details about the actual raster size. The target fan speed was fixed at 60 Hz. A similar study was carried out for a 4 mm × 4 mm raster and also for the liquid deuterium (LD$_2$) cell, but those results are not presented here.

2 Beam Properties

The beam raster size was measured by the stripline BPMs to be 1.98 mm × 2.10 mm (horizontal × vertical) taken at the points where the distribution falls

to 10% of the peak height (relative to the corresponding peak – there are two peaks in the beam position distribution for the rectangular raster). These values are the averages over all the runs included in this study though there is very little variation about these average values. However, we now believe the BPMs to be systematically off for rastered beams. This was revealed by data with rastered beam on a thin foil with the foil's normal along the beam direction. A correlation between the vertex position along the beam direction (referred to hereafter as "reactz") measured using either of the two spectrometers and the horizontal position measured using the BPMs was noted. The correlation could be removed by multiplying the measured beam position by a factor of roughly 1.3. Note this factor fixed the correlations observed with both spectrometers. Based on this observation and on an earlier study of the BPMs [3], we believe the beam size should be corrected by a factor of 1.3 and 1.2 for the horizontal and vertical coordinates respectively. Using these factors, our estimate for the actual size of the beam during our study is 2.6 mm × 2.5 mm (horizontal × vertical).

While the intrinsic beam spot size (*i.e.* the size without rastering) might also affect the LH_2 density, we had no good measure of this during this study. The encoder for the HARP6 scanner (HARP6 is the scanner closest to the target) was unfortunately switched off and finally restored during a four hour machine development period following the LH_2 density study. However, two HARP scans using the HARP5 scanner, further upstream from the target, were performed, one 7 hours before and one 15 hours after the density measurements. They revealed the spot size (horizontal by vertical σ widths) to be 64 μm × 72 μm and 80 μm × 56 μm, respectively.

3   Data Analysis

The runs used for this study (performed in October 2002) were numbered 2615–2617, 2619–2623 and 2625 with the beam current ranging from 111.2 μA down to 5.3 μA. Accelerator performance was unusually poor during this period as judged by the large number of beam trips for these runs. This complicated the analysis since only the portion of the runs with steady current could be utilized. It was therefore necessary to remove data for a time interval following the start and preceding the end of each steady beam period [4] causing a small loss of statistical precision.

The raw data files were scanned to establish the average beam current between successive scaler reads. The beam was considered "steady" for all contiguous portions of a run with beam currents deviating by no more than 2 μA between any two successive scaler reads. Further, the first 20 seconds of each such period was removed to avoid any time-dependent effects. This resulted in a file containing event number pairs defining each such period used to condition subsequent analysis as well as various scaler sums for each period needed for data normalization.

The data were analyzed with ESPACE cutting on the portions of each run with steady beam current. No other cuts were placed on the analysis at this

Run	Current (μA)	CLT1	CLT3	CLT5	TrEff1	TrEff3	TrEff5
2615	111.20	0.9517	0.9555	0.9430	0.985	0.933	0.983
2616	100.21	0.9547	0.9577	0.9464	0.986	0.935	0.980
2617	80.37	0.9616	0.9641	0.9555	0.985	0.935	0.983
2619	60.35	0.9624	0.9637	0.9573	0.986	0.935	0.982
2620	40.78	0.9727	0.9735	0.9682	0.987	0.935	0.984
2621	19.99	0.9728	0.9708	0.9762	0.988	0.937	0.985
2622	10.05	0.9783	0.9793	0.9779	0.989	0.939	0.990
2623	9.14	0.9875	0.9862	0.9911	0.989	0.938	0.983
2625	5.27	0.9784	0.9759	0.9804	0.989	0.936	0.986

Table 1: Beam current, computer livetime and tracking efficiency for trigger types T1, T3 and T5 for each run.

level. The output of this analysis was an HBOOK Ntuple for each run. The "ts_patt" variable, which identifies the active trigger(s) at the Trigger Supervisor, was included in the Ntuples in order to examine the target density for electron singles (^{1}H(e, e')), proton singles (^{1}H(e, p)) and coincidence (^{1}H($e, e'p$)) triggers. In our experiment, the electron spectrometer was on beam left (trigger "T3") and the proton spectrometer was on beam right (trigger "T1"). (Here "left" and "right" refer to the directions as seen viewing downstream.) Coincidence triggers are referred to as "T5".

4 Computer and Electronic Deadtimes

After analyzing the data for the three trigger types, normalization factors were determined allowing correction for beam charge and computer deadtime. The computer deadtime was never more than 6% for any of the trigger types (see Table 1).

No correction was made for electronic deadtime as the single-arm trigger rates were always less than 1 kHz (before prescaling), even for the highest beam current (see Table 2).

5 VDC Cuts and Tracking Efficiency

The data were analyzed with VDC cuts such that only events with three or more hits in each wire plane (four planes for the single-arm triggers and eight for the coincidence triggers) and one track (for coincidence triggers this means exactly one track in each spectrometer) were considered. In addition, for each spectrometer a cut on particle velocity, β, was enforced, eliminating the region around the cosmic ray peak ($\beta = -1$). The data were then corrected for "tracking efficiency" by multiplying the resulting spectra by the ratio of events of a given trigger type with three or more hits to those with three or more hits and exactly one track. Both of these numbers were conditioned on the β cut. This correction was fairly small and nearly constant for a given trigger type for the

3

Run	Current (μA)	T1 Rate (Hz)	T3 Rate (Hz)	T5 Rate (Hz)
2615	111.20	642	829	218
2616	100.21	596	768	203
2617	80.37	508	647	177
2619	60.35	401	503	142
2620	40.78	279	346	101
2621	19.99	142	171	52
2622	10.05	75	91	28
2623	9.14	69	83	25
2625	5.27	43	52	16

Table 2: Trigger rates (before prescaling).

various runs (see Table 1). The difference between so correcting and simply using all the tracked data without any VDC cuts or corrections was completely negligible, at least for the extraction of the dependence of the target density on beam current. In addition, the difference between imposing no upper limit on the per plane multiplicities and requiring no more than 10 hits per plane was completely negligible.

6 Other Cuts

In addition to the raw VDC cuts and β cuts mentioned above, a cut on the vertex (reactz) was imposed: $|$reactz$|$ < 0.05 m. Beyond this the cell walls had substantial influence on the results. We plan to use this same cut for the production data on deuterium.

For the electron single-arm data the invariant mass of the final hadronic system (*i.e.* W) was cut between 0.930 GeV and 0.970 GeV. For the coincidence data, the missing mass (*i.e.* "e_miss") was cut between -8.0 MeV and $+8.0$ MeV. These cuts are quite effective in eliminating contributions from all sources except the target liquid. For the proton single-arm data a cut was placed on the correlation between scattering angle and momentum (*i.e.* ph_tg and dp) to reduce the contribution due to inelastic scattering. This cut is not as clean as the cuts for the other trigger types, and so an additional cut on the r-function[5] value was made: $r > 0.005$. This could be especially important since we used the "open" collimator setting for both spectrometers. However, the results were very insensitive to any of these cuts (except for reactz - see below), lending credence to the extraction of the target density dependence.

7 Results

The normalized rates for each trigger type as a function of beam current are shown in Figure 1 along with linear fits for the high current ($\geq$ 40 μA) runs. The rates for runs with currents below 40 μA are consistent with a constant,

4

Trigger	Current Range (μA)	Slope (μA^{-1})
T1	< 40	0.6720E-03 ± 0.1033E-02
T3	< 40	0.3579E-03 ± 0.7001E-03
T5	< 40	-0.6824E-03 ± 0.1579E-02
T1	≥ 40	-0.2761E-02 ± 0.1340E-03
T3	≥ 40	-0.2561E-02 ± 0.9088E-04
T5	≥ 40	-0.2733E-02 ± 0.1841E-03

Table 3: Slopes of normalized trigger rates *vs.* current for the three trigger types. The regions below and above 40 μA employed separate linear fits.

indicating no significant density reduction at low current. (This qualitative behavior was also found from another study performed immediately following our experiment using "lumi" monitors [6]. See the lower left panel of Figure 14 in that paper.) The slopes and their uncertainties are given in Table 3 for both the low and high current runs. Extractions from all three trigger types (T1, T3 and T5) are reasonably consistent with one another.

The extraction of the target density dependence is quite sensitive to the cut on reactz (there is no *a priori* reason to expect the target density to be independent of the z position). Therefore the reactz dependence was examined in detail. Since the shape of the reactz distribution depends on details of the acceptance and physics weighting (through correlations between reactz and angle of the exiting particles) one cannot draw conclusions about the target density distribution from a single reactz spectrum. To remove these unwanted dependences the reactz spectrum for each beam current was compared to those from runs taken at low current. For each run, the normalized reactz spectrum was divided by the average (in order to minimize statistical variations) of the reactz spectra for the four lowest beam currents (all ≤ 20 μA). This was done independently for each trigger type (T1, T3 and T5). The ratio spectra so obtained should be relatively independent of acceptance and physics effects. The results are shown in Figures 2, 3 and 4 respectively for T1, T3 and T5 triggers. A few observations can be made. All ratio spectra are very close to unity at the left edge of the considered reactz acceptance (*i.e.* for −0.05 m). (Beyond the ± 0.05 m considered here, the spectra oscillate, presumably due to effects from the target cell walls.) This implies that there is very little density reduction at the target entrance, even for the highest beam current used. The slopes decrease with decreasing current, as expected. The density reduction becomes small and consistent with zero as the beam current drops below 40 μA or so, which can also be seen from Figure 1.

For each trigger type, the dependence of the slopes of the ratio histograms on beam current were examined. Linear fits to the nine slopes shown in the previous three figures were performed and the results are shown in Figure 5. The values of the slopes for both high and low current regions are given in Table 4. These
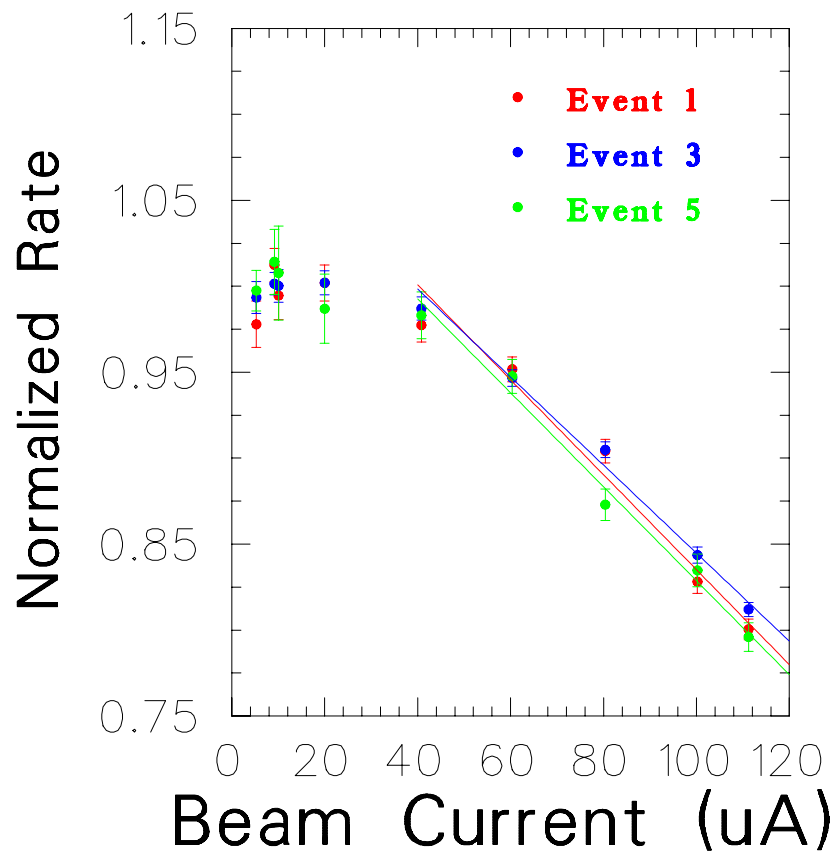
Figure 1: The normalized rates, corrected for beam charge, computer deadtime and VDC tracking efficiency, for each trigger type as a function of beam current. Also shown are the results of linear fits for the high current ($\geq 40 \ \mu A$) runs.
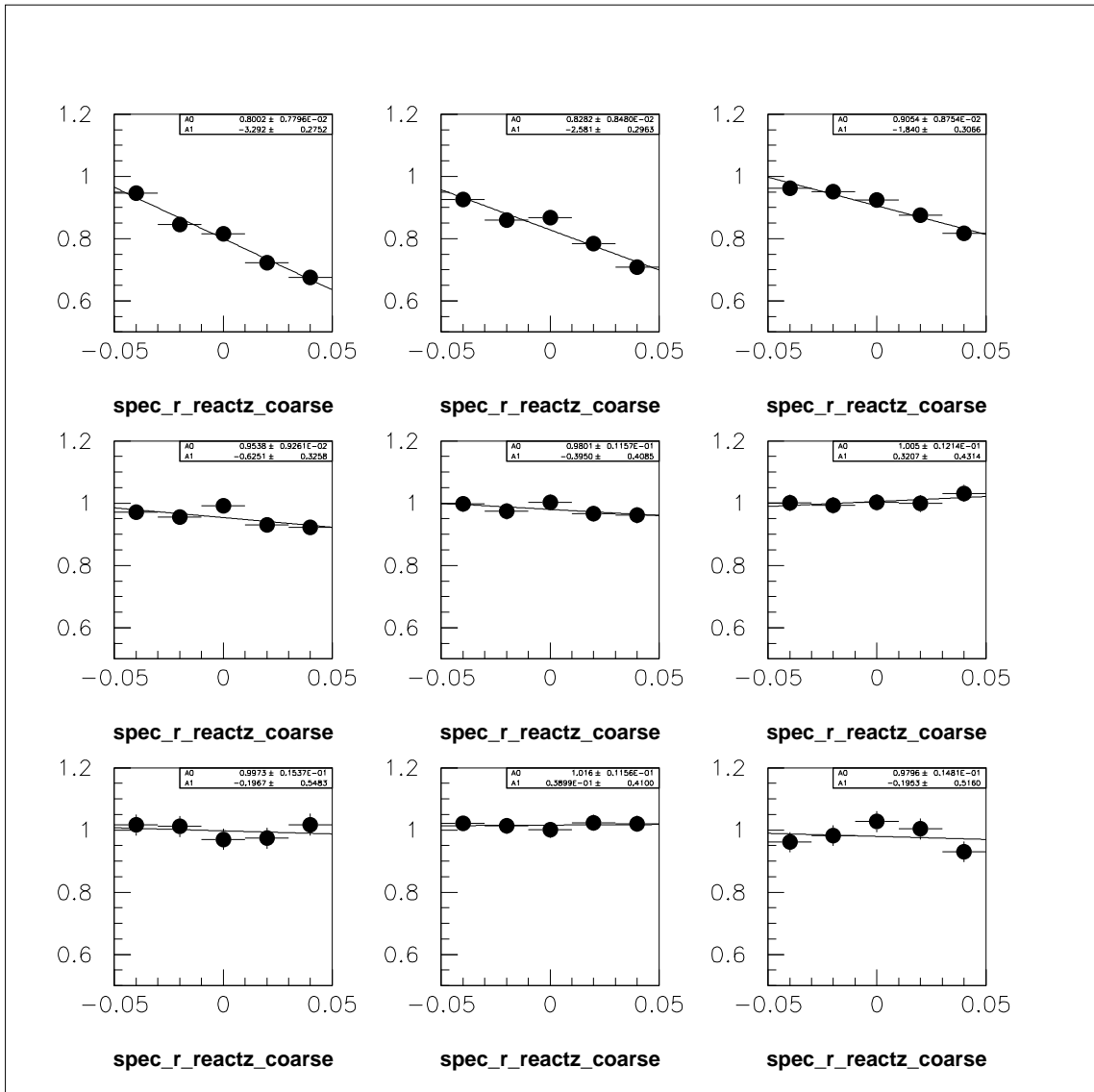
Figure 2: The normalized reactz spectra for T1 triggers for each of the nine runs used in the analysis. Each spectrum has been divided, channel by channel, by the average of the lowest four current runs. The current decreases monotonically reading left-to-right and down the page.
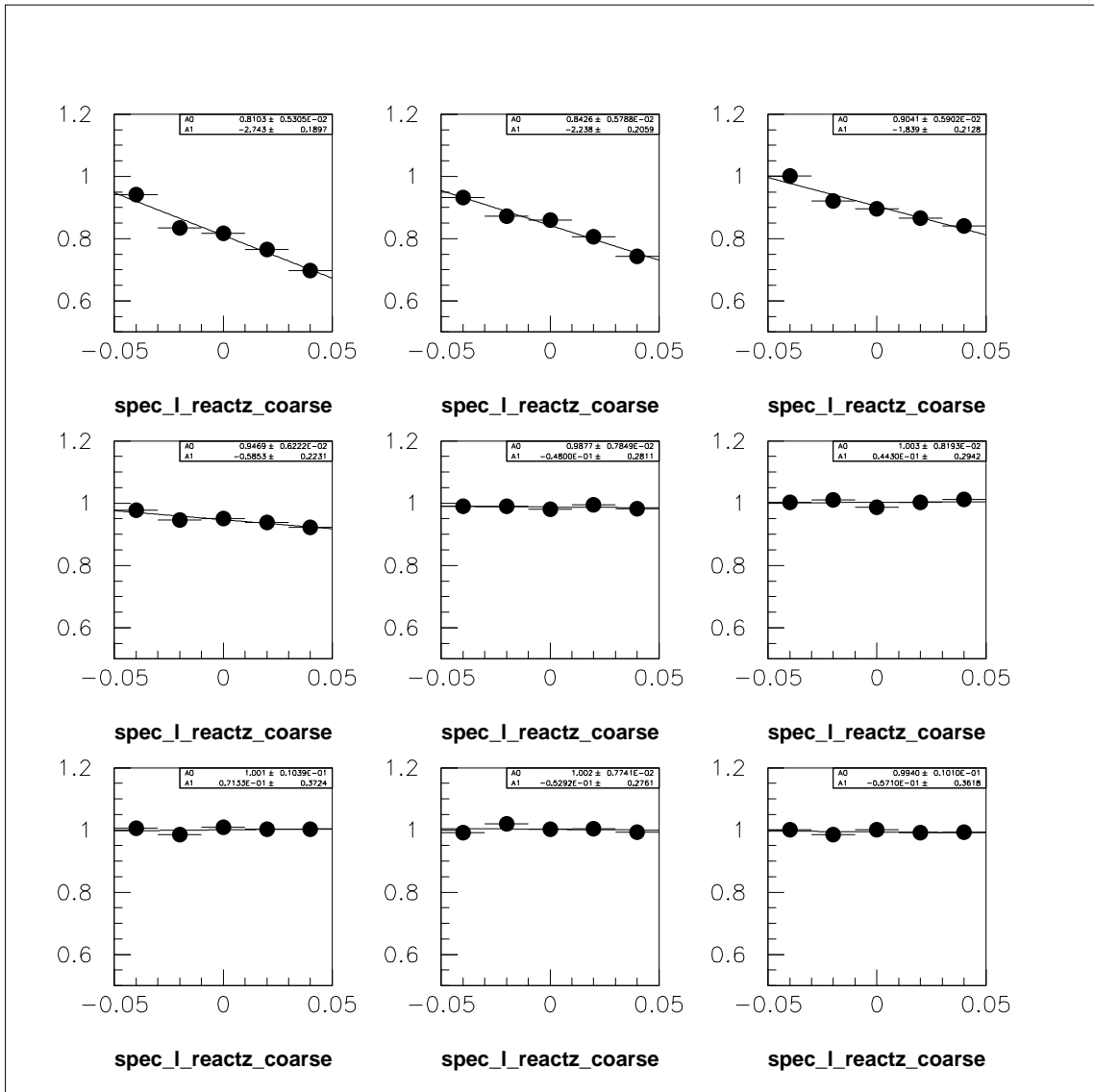
7

Figure 3: The normalized reactz spectra for T3 triggers for each of the nine runs used in the analysis. Each spectrum has been divided, channel by channel, by the average of the lowest four current runs. The current decreases monotonically reading left-to-right and down the page.
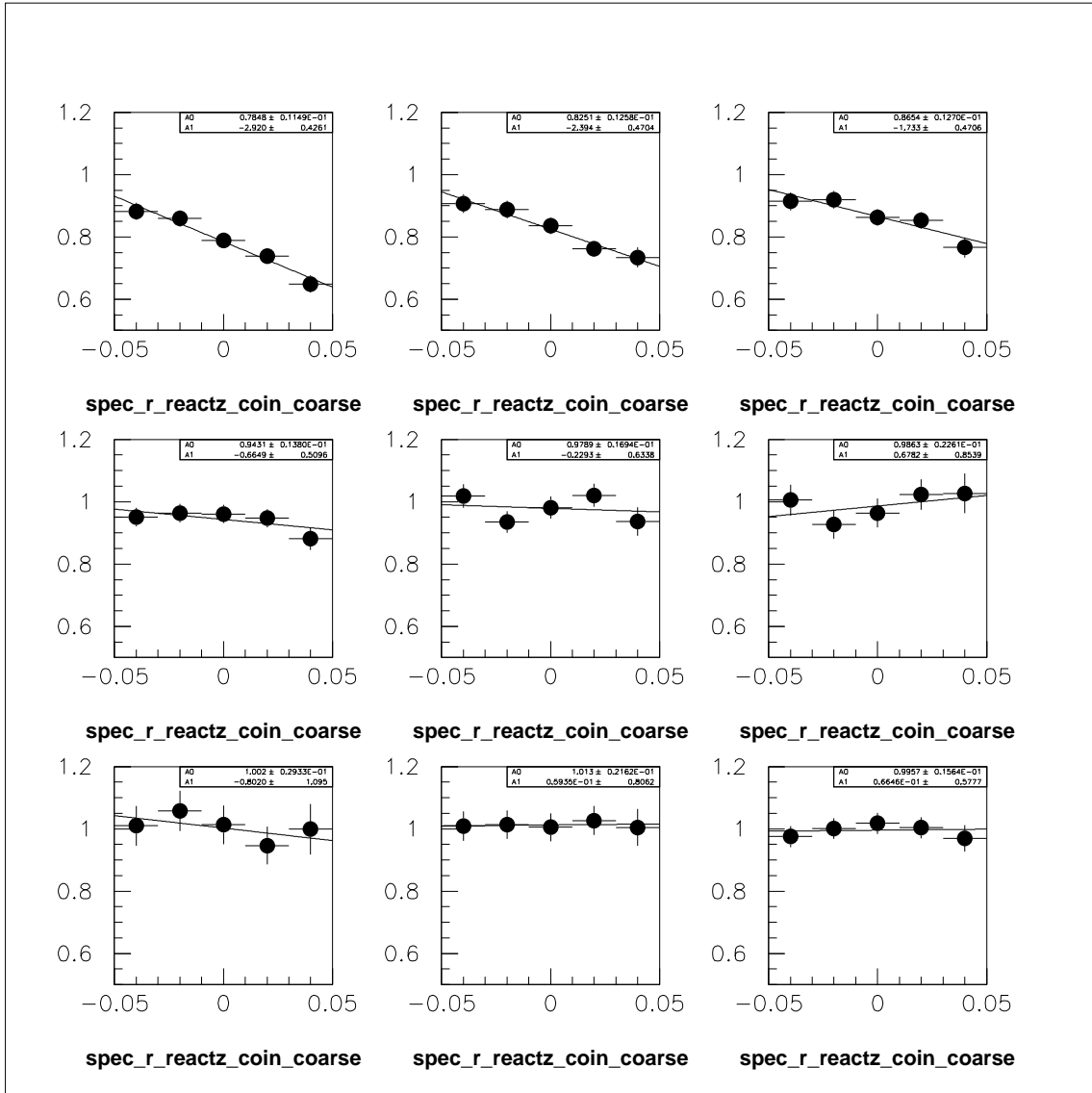
8

Figure 4: The normalized reactz spectra for T5 triggers for each of the nine runs used in the analysis. Each spectrum has been divided, channel by channel, by the average of the lowest four current runs. The current decreases monotonically reading left-to-right and down the page.

9

Trigger	Current Range (μA)	α ($[\mu\text{A-meter}]^{-1}$)
T1	< 40	0.3404E-01 +/- 0.4177E-01
T3	< 40	0.6562E-02 +/- 0.2867E-01
T5	< 40	0.4095E-01 +/- 0.6988E-01
T1	≥ 40	-0.4429E-01 +/- 0.5836E-02
T3	≥ 40	-0.3902E-01 +/- 0.4019E-02
T5	≥ 40	-0.3999E-01 +/- 0.9082E-02

Table 4: Slopes with respect to beam current of the reactz slopes for the normalized trigger rates *vs.* for the three trigger types. The regions below and above 40 μA were fit separately.

"double slopes" (referred to as α in Table 4) are consistent for all three trigger types. Further, they are consistent with zero for the low current region.

For beam currents ≥ 40 μA, we can parameterize the density of the LH$_2$ target fluid as:

$$\rho(z, I) = \rho_0 \left[1 + \alpha(z - z_0)(I - I_0)\right] \quad \text{for } I \geq 40 \mu\text{A} \tag{1}$$

and as a constant (ρ_0) for currents below 40 μA. Here, ρ_0 is the density of the target fluid in the absence of beam, z is the value of reactz in meters, $z_0 = -0.05$ m, I is the beam current in μA and $I_0 = 40\,\mu$A. The values of α are given in the last three columns of Table 4 for each of the three trigger types. Taking the weighted average over trigger types, we get:

$$\alpha = -0.0406 \pm 0.0031 \tag{2}$$

From this relation we can estimate, for example, the density reduction at the center of the target ($z = 0$) which is equal to the overall reduction for any distribution symmetric about the target center. For a beam current of 100 μA this amounts to: $\rho = 0.878\,\rho_0$ with an uncertainty of 0.9%. Note this uncertainty includes the statistical uncertainties and fit parameter uncertainties, weighted over the three trigger types.

8 Summary and Conclusions

For beam currents above 40 μA, the liquid hydrogen in the cigar-tube cell shows substantial density variation, both with beam current and position along the beam, at least for the 2 mm $\times$ 2 mm rastered beam used in this study. Separate linear fits below and above 40 μA describe both the beam current and z dependences well, leading to the simple parameterization given above. Results for the three trigger types (Left spectrometer, Right spectrometer and coincidence) are consistent with one another, at least for the parameterization given. For distributions which sample z symmetrically about the target center, the density reduction is 12.2 ± 0.9 % at a beam current of 100 μA. This value is reasonably consistent with another study using "lumi" monitors [6].
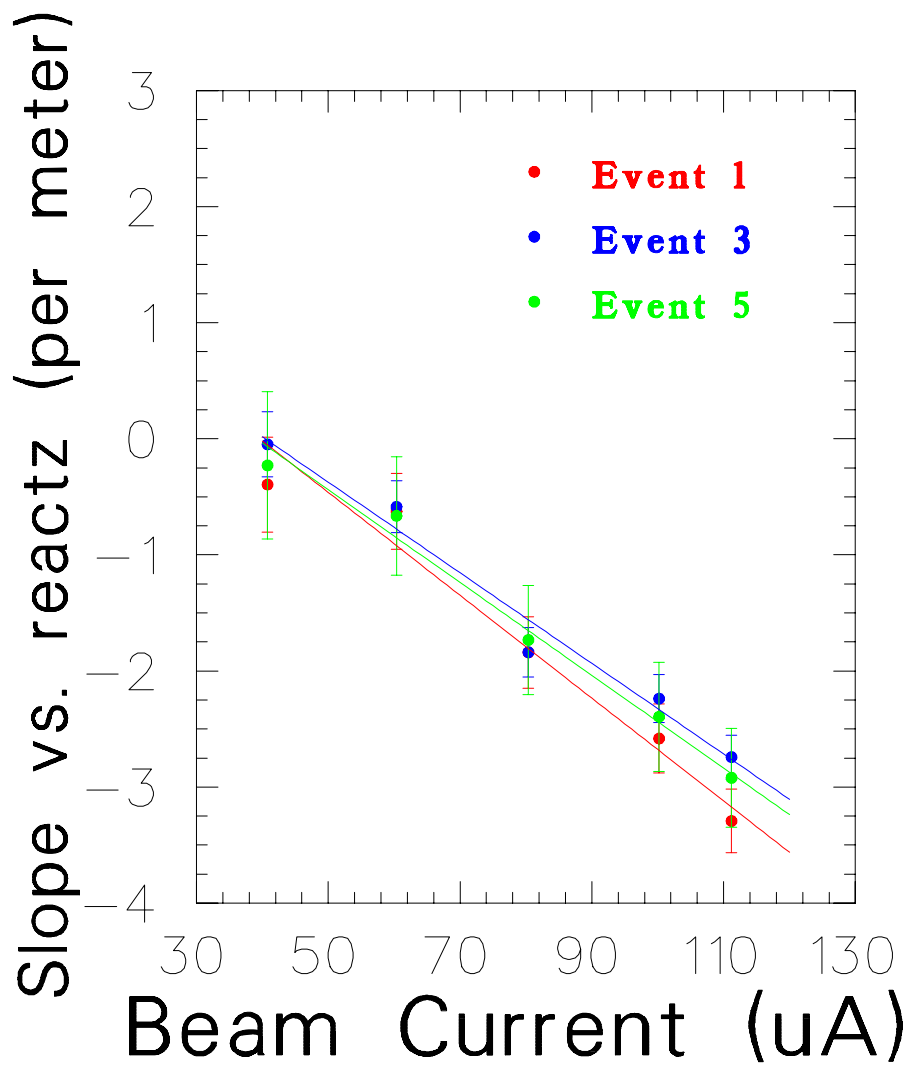
Figure 5: The slopes *vs.* reactz for each trigger type as a function of beam current for currents $\geq 40\ \mu$A along with linear fits.

While our results are consistent with no density reduction below currents of 40 μA, due to the statistical uncertainties of our data we cannot rule out the small reduction seen in the lumi monitor study at low currents. Nonetheless, there seems to be a significant change in the slope of density *vs.* current occurring near 40 μA. One possible explanation is that the onset of boiling begins near this current, while smaller density changes occur at lower currents due to an increase of the liquid temperature.

Additional data were taken with a 4 mm × 4 mm rastered beam, but were not analyzed here. It might be of interest to repeat this analysis for the larger raster, though the production data employed only the 2 mm × 2 mm rastered beam. Obviously, results for the LD_2 target would be of interest to this experiment and are being examined by other members of the collaboration [7].

9 Acknowledgements

10 References

[1] JLab Experiment E01-020, W. Boeglin, M.K. Jones, A. Klein, P.E. Ulmer and E. Voutier, cospokespersons.

[2] J.Alcorn *et al.*, *Nucl. Instr. Meth. A* **522**, 294 (2004).

[3] *Beam Position Studies for E93050*, C. Hyde-Wright, L. Todor and G. Laveissiere, JLab-TN-01-001 (2001).

[4] Software tools to determine the steady beam portions of each run and to produce corresponding cut files for ESPACE were created by H. Ibrahim and L. Coman, the graduate students on this experiment.

[5] V.L. Rvachev, T.I. Sheiko, V. Shapiro and I. Tsukanov, *Comp. Mech.* **25**, 305 (2000).

[6] *Target Density Fluctuations and Bulk Boiling in the Hall A Cryotarget*, D.S. Armstrong, B. Moffit, and R. Suleiman, JLab-TN-03-017 (2003).

[7] Analysis to extract the LD_2 target density is being carried out by L. Coman of Florida International University.